Follow us @BoneJointRes

Freely available online OPEN ACCESS

BJR

MUSCLE & TENDON

Effect of secretory leucocyte protease inhibitor on early tendon-to-bone healing after anterior cruciate ligament reconstruction in a rat model

Y. Wu,
Y. Shao,
D. Xie,
J. Pan,
H. Chen,
J. Yao,
J. Liang,
H. Ke,
D. Cai,
C. Zeng

From The Third Affiliated Hospital of Southern Medical University, Guangzhou, China

Aims

To verify whether secretory leucocyte protease inhibitor (SLPI) can promote early tendon-to-bone healing after anterior cruciate ligament (ACL) reconstruction.

Methods

In vitro: the mobility of the rat bone mesenchymal stem cells (BMSCs) treated with SLPI was evaluated by scratch assay. Then the expression levels of osteogenic differentiation-related genes were analyzed by real-time quantitative PCR (qPCR) to determine the osteogenic effect of SLPI on BMSCs. In vivo: a rat model of ACL reconstruction was used to verify the effect of SLPI on tendon-to-bone healing. All the animals of the SLPI group and the negative control (NC) group were euthanized for histological evaluation, micro-CT scanning, and biomechanical testing.

Results

SLPI improved the migration ability of BMSCs and upregulated the expression of genes related to osteogenic differentiation of BMSCs in vitro. In vivo, the SLPI group had higher histological scores at the tendon-bone interface by histological evaluation. Micro-CT showed more new bone formation and bone ingrowth around the grafted tendon in the SLPI group. Evaluation of the healing strength of the tendon-bone connection showed that the SLPI group had a higher maximum failure force and stiffness.

Conclusion

SLPI can effectively promote early tendon-to-bone healing after ACL reconstruction via enhancing the migration and osteogenic differentiation of BMSCs.

Cite this article: *Bone Joint Res* 2022;11(7):503–512.

Keywords: Secretory leucocyte protease inhibitor, Tendon-bone healing, Osteogenic differentiation, Anterior cruciate ligament reconstruction

Article focus

- We aimed to identify the effect of secretory leucocyte protease inhibitor (SLPI) on tendon-bone healing after anterior cruciate ligament (ACL) reconstruction in rats through in vivo and in vitro experiments, and to investigate the preliminary mechanism.

Key messages

- SLPI has been shown to have a significant osteogenesis-promoting effect.
- Superior and firm tendon-bone healing is dependent on new bone formation and ingrowth around the grafted tendon.

Strengths and limitations

- Both in vivo and in vitro experiments were conducted.
- Comprehensive evaluation of the effect of SLPI on tendon-bone healing in rats was conducted via various methods such as histological assessment, micro-CT scanning, and biomechanical testing.

Correspondence should be sent to Chun Zeng; email: zengdavid@126.com

doi: 10.1302/2046-3758.117.BJR-2021-0358.R2

Bone Joint Res 2022;11(7):503–512.

- Limitations include a superficial investigation of molecular mechanisms of SLPI in promoting tendon-bone healing process, and small animal models, which cannot fully simulate the tendon-bone healing process in humans.

Introduction

Anterior cruciate ligament (ACL) reconstruction is one of the most common orthopaedic procedures.[1-3] However, there are some problems such as "wiper effect" (transverse graft motion by extracortical femoral fixation) and "bungee effect" (longitudinal graft motion by extracortical femoral fixation) after the operation, which often lead to tunnel widening and joint laxity. Poor healing of the tendon-bone repair in the early stage is a critical cause of ACL reconstruction failure.[4] Therefore, exploring how to improve early tendon-bone healing is very important for ACL reconstruction.

Previous studies have confirmed that successful ACL reconstruction depends on good osseointegration between the tendon graft and the bone tunnel. Among them, bone mesenchymal stem cells (BMSCs) play an important role in the process of tendon-bone healing.[4,5] BMSCs are mesenchymal stem cells with multidifferentiation potential and have been increasingly used as a cell source for tissue repair research in recent years.[6-8] In addition, the ability of BMSCs to differentiate into osteoblasts has been confirmed, which undoubtedly plays an important role in the process of tendon-to-bone healing.[9] Therefore, it is critical to find methods of promoting and enhancing the effects of BMSCs. Studies have proved that superior tendon-to-bone healing depends on the process of new bone ingrowth, mineralization, and maturation around the bone tunnel,[10] so it is very important to find a factor that can promote osteogenic differentiation at the tendon-bone interface.

Secretory leucocyte protease inhibitor (SLPI), a serine protease inhibitor, belongs to the whey acidic protein family and is secreted and expressed by macrophages, epithelial cells, and neutrophils of multiple tissues and organs.[11] With protease-inhibiting, anti-inflammatory, antibacterial, and antiviral activities, and growth regulation, SLPI has been broadly studied in many fields such as wound repair, infection, growth, and cell proliferation.[12-14] In addition, studies suggest that SLPI is associated with bone formation[15] and cell migration.[16]

Therefore, it is our hypothesis that SLPI may enhance early tendon-to-bone healing by promoting the migration and osteogenic differentiation of BMSCs.

Methods

Cell culture and scratch assays. Rat BMSC lineages were purchased from Cyagen (USA). The third generation of the cell lineage was maintained in complete α-Minimum Essential Medium (MEM) (Thermo Fisher Scientific, USA) containing 10% fetal bovine serum. The cells were incubated at 37°C, in a 5% carbon dioxide atmosphere, and observed periodically to ensure the cells retained their shuttle-shaped morphology. Cells were passaged when they reached 80% confluence. The methods were as follows: BMSCs were seeded into six-well plates and a scratched area was created using a 200 µl pipette tip when the cells reached 100% confluence. The wells were washed three times in phosphate-buffered saline to remove floating cells, and the remaining cells were cultured in serum-free medium,[17] with the addition of r-SLPI (AtaGenix, China) at 1 µg/ml[18] to the SLPI group while the NC group was not treated. Photographs were taken under a phase-contrast microscope (Olympus) at zero and 24 hours post-scratching, to observe movement of the cells. The experiment was repeated three times, and migration ability was determined by the scratch healing rate evaluated by ImageJ (National Institutes of Health, USA). Scratch repair rate (%) = (original scratch area – scratch area after 24 hours)/original scratch area.[19,20]

Osteogenic induction and qPCR. BMSCs were cultured in osteogenic induction medium (PythonBio) consisting of α-MEM, 50 µM ascorbic acid, 10 mM β-glycerophosphate, 100 nM dexamethasone, and 10% fetal bovine serum (Thermo Fisher Scientific). The SLPI group was treated with r-SLPI at 1 µg/ml,[18] while only changes of osteogenic induction medium were performed in the NC group. Total RNA was extracted from cells using Total RNA Extraction Reagent (Vazyme, China) after seven or 14 days of induction. RNA concentration was measured using a microplate reader. Complementary DNA was synthesized using the HiScript II Q RT SuperMix transcription kit (Vazyme), and finally, reverse transcription quantitative polymerase chain reaction (RT-qPCR) was performed using ChamQ SYBR qPCR Master Mix (Vazyme) in a thermal cycling instrument. Data were analyzed with the 2-ΔCt method and all experiments were repeated in triplicate. The primer sequences used are shown in Table I.

Animal study design and surgical procedure. All operations followed the rules of the Institutional Animal Care and Use Committee. An ARRIVE checklist is included in the supplementary material to show that the ARRIVE guidelines were adhered to in this study. A total of 36 adult male Sprague-Dawley rats (280 g to 320 g weight) purchased from Southern Medical University (Guangzhou, China) were randomly divided into two groups (18 per group): the negative control (NC) group (fibrin gel injection alone) and the SLPI group (fibrin gel loaded with recombinant SLPI (rSLPI) protein). The surgical procedures were performed as previously described.[21,22] Briefly, a rat unilateral ACL reconstruction model was used. After successful general anaesthesia with an intraperitoneal injection of pentobarbital sodium solution (20 mg/kg), a medial right ankle incision was made to harvest the flexor digitorum longus tendon (Figures 1a and 1b). Another medial parapatellar incision was made, the patella was laterally dislocated, and the native ACL was identified and removed (Figure 1c). Bone tunnels were established in the femur and tibia through the footprints of the intrinsic ACL with a 1.0 mm drill (Figure 1d). After pulling the flexor digitorum longus tendon into the bone tunnels

Table I. Primers for the genes associated with osteogenic differentiation.

Target	Forward	Reverse
Runx2	5'-CGCCTCACAAACCACAG-3'	5'-AATGACTCGGTTGGTCTCGG-3'
OCN	5'-CAACCCCAATTGTGACGAGC-3'	5'-AACGGTGGTGGCATAGATGC-3´
ALP	5'-GTTTTCTGTTCTGTAAGACGGG-3'	5'-GCCGTTAATTGACGTTCCGA-3´
OPN	5'-GGCTTACGGACTGAGGTCAA-3'	5'-AGGTCCTCATCTGTGGCATC-3´
GAPDH	5'-TAGCAACTTTGGCATCGTGG-3'	5'-GGGCCATCCACAGTCTTCTG-3´

ALP, alkaline phosphatase; GAPDH, glyceraldehyde-3-phosphate dehydrogenase; OCN, osteocalcin; OPN, osteopontin; Runx2, runt-related transcription factor 2.

(Figure 1e), each tunnel of the knee in the SLPI group was injected evenly around the tendon graft with 0.1 ml fibrin gel containing 1 µg r-SLPI (release kinetics of SLPI from fibrin gel as shown in Supplementary Figure a), while the NC group was treated with fibrin gel injection only. Both ends of the graft were fixed onto the periosteum of the femur and tibia with a 2-0 absorbable Ethibond suture (Johnson & Johnson, USA) with the knee in 30° of flexion. Finally, after repositioning the patella, the joint capsule and skin were sutured in layers to complete the operation (Figure 1f). All the animals were allowed to move freely in their cages after ACL reconstruction. Animals were administered 80,000 U of penicillin by intraperitoneal injection for three consecutive days after surgery, and the wounds and general conditions of the animals were examined daily. No animal deaths or infections occurred during our study, so no animals were excluded.

Specimen collection and preparation. At two, four, and eight weeks after ACL reconstruction, the animals in each group were euthanized by inhalation of excess carbon dioxide. Micro-CT scanning (n = 4) was performed immediately after this, followed by harvesting tissue samples, which were placed in decalcifying solution after fixation with 10% formaldehyde for 72 hours at 4°C. The samples were paraffin-embedded until used for histological staining and immunohistochemistry (IHC, n = 4). Additionally, the samples were taken from the animals at eight weeks postoperatively, six samples from each group were subjected to direct biomechanical testing, and no further histological evaluation would be performed on samples that had undergone biomechanical testing.

Micro-CT scans and analysis. The operated limbs (four per group) were harvested from all the rats at each timepoint following euthanasia and fixed in the scanning tubes. A five-minute pre-scan was performed with a micro-CT scanner (Scanco Medical, Switzerland), with the following parameters: resolution: 30 µm, voltage: 55 KVp, current: 145 µA, and energy: 8 W. Scanning was performed from the tibial plateau to the distal exit of the tibial tunnel for about 30 minutes. After scanning, a region of interest with a diameter of 1.5 mm and a height of 5 mm was selected from the tibial plateau to distal tibia, and the bone volume/total volume (BV/TV) and bone mineralization density (BMD) were analyzed. Cross-sectional images of the tibial bone tunnel, at a depth of 1.5 mm below the tibial articular surface, were measured.[21]

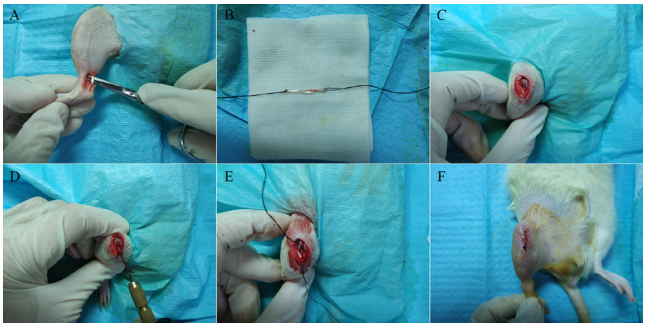

Fig. 1

a) and b) To create a rat model of anterior cruciate ligament (ACL) reconstruction, the rat was placed in the supine position and the flexor digitorum longus tendon was freed under aseptic conditions. c) A medial patellar incision was made to expose the knee joint and the intrinsic ACL was removed. d) A femoral tunnel was created with a drill (1 mm diameter). e) After femoral and tibial tunnels were established, both ends of the transplanted tendon were fixed and pulled into the bone tunnels. f) The incisions were sutured after injection of fibrin gel with or without recombinant secretory leucocyte protease inhibitor around the graft tendon, and the operation was completed.

Biomechanical testing. Animals were euthanized at eight weeks after ACL reconstruction. The specimens (six per group) were harvested for biomechanical testing immediately, in accordance with the methods outlined in a previous study.[23] Briefly, before testing, the fixed sutures around the tendon and the soft-tissue were carefully removed, and only the femur-graft-tibia complex was preserved and subjected to testing by a high-precision biomaterial testing system (ELF-3510AT; Bose Corporation, USA). The femur and tibia were fixed with clips (Figure 2a). Tensile force was applied along the axis of the grafted tendon. The complex was stressed with a pre-tensile force of 1 N for five minutes and then underwent testing with an elongation rate of 0.5 mm/s until the tendon was pulled out or ruptured. The maximum load force was recorded at tendon failure, and tension-deformation curve was simultaneously recorded by the testing system. The stiffness was calculated from the slope of the highest point of the curve.

Histological evaluation. Before histological staining/IHC analysis, the paraffin-embedded samples were sectioned using a microtome (Leica tissue slicer; Leica Microsystems, Germany) vertically to the longitudinal axis of the transplanted tendon with a thickness of 5 µm. The sections were stained with haematoxylin and eosin

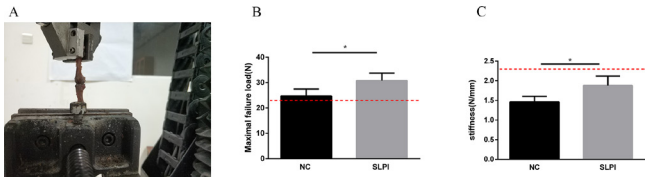

Fig. 2

a) Biomechanical testing performed using a biomaterial testing system. b) Maximum tensile force and c) stiffness of the secretory leucocyte protease inhibitor (SLPI) group and the negative control (NC) group were recorded. Both the maximum tensile force and stiffness were higher in the SLPI group. Results are presented as mean and standard deviation (n = 6), *p < 0.05. The red dashed line in b) and c) indicates maximum failure tension and stiffness of the intact anterior cruciate ligament.

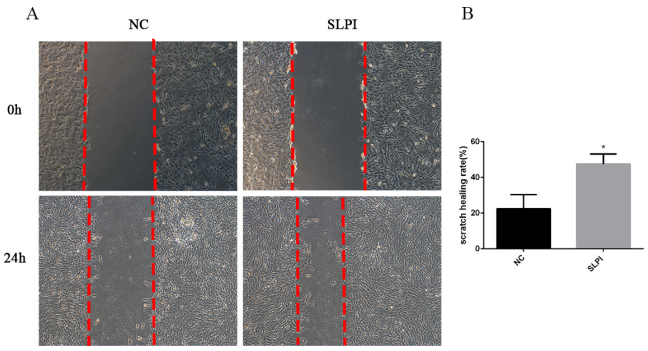

Fig. 3

Scratch assay was performed to evaluate cell migration (n = 3). a) Images of the secretory leucocyte protease inhibitor (SLPI) group show a small scratch area at 24 hours after addition of SLPI. b) Quantification of the scratch healing rate based on a). NC, negative control. *p < 0.05.

(H&E), Masson's trichrome, and modified Safranin O/Fast green staining. The sections were examined blindly and independently by three observers (DX, YS, JY), who selected and examined it to assess fibrocartilage formation, new bone formation, and tendon graft bonding to adjacent tissues according to the scoring system (Table II).[24] IHC staining for Runx2 (Rabbit-derived; Abcam, USA) and OCN (Rabbit-derived; Proteintech, China) were used to detect osteogenic differentiation-related indicators at the tendon-bone interface of serial tissue sections. Antigen heat retrieval was performed after dewaxing and hydration. Endogenous peroxidase was eliminated with 3% hydrogen peroxide. Normal goat serum was used to block non-specific antigens, then sections were incubated with the appropriate primary antibody (Runx2: 0.52 mg/ml, OCN: 0.8 mg/ml) overnight at 4°C followed by the secondary antibody (Goat-derived; ImmunoWay, China; 4 mg/ml) for one hour at room temperature. Finally, the diaminobenzidine solution was prepared to detect positively stained cells. After IHC staining, the sections were observed and evaluated by three independent researchers (DX, YS, JY). The results are expressed as the number of positive cells as a proportion of the total number of cells per high-power field (magnification × 400). All

Table II. Scoring system for histological results.[24]

Characteristic	Points
Fibrocartilage formation	
Abundant	3
Moderate	2
Slight	1
None	0
New bone formation	
Abundant	3
Moderate	2
Slight	1
None	0
Tendon graft bonding to adjacent tissue	
75% to 100%	3
50% to 75%	2
25% to 50%	1
0% to 25%	0

sections were photographed under a light microscope (Olympus, Japan).

Statistical analysis. All data are expressed as mean and standard deviation (SD), and were analyzed using SPSS statistics software (version 20.0, IBM, USA). The statistical differences between the two groups at each timepoint were compared using the independent-samples *t*-test. p-values < 0.05 were considered statistically significant.

Results

BMSCs migration capacity. To clarify the effect of SLPI on BMSCs, a scratch assay was used to examine cell migration ability. The results showed that overexpression of r-SLPI significantly increased the mobility of BMSCs compared to the NC group (Figure 3a). The scratch area healing rate was dramatically higher after 24 hours in the SLPI group (p = 0.011) (Figure 3b).

Osteogenic differentiation-related gene expression. The expression of osteogenic differentiation-related genes (*Runx2*, *ALP*, *OCN*, and *OPN*) was examined by qPCR after induction of BMSCs in osteogenic differentiation medium for seven or 14 days, and the results showed (Figure 4) that the expression of *Runx2* and *ALP* in BMSCs was significantly increased in the SLPI group at seven (p < 0.001 and p = 0.009, respectively) and 14 (p = 0.012 and p = 0.013, respectively) days of induction; there was no difference in the expression of *OCN* and *OPN* between the two groups at day 7 of induction, but expressions in the SLPI group were significantly upregulated compared with the NC group at 14 days (p = 0.006 and p = 0.005, respectively).

Expression of osteogenesis-related markers at the tendon-bone interface. Expression of the osteogenic differentiation-related protein markers Runx2 and OCN at the tendon-bone interface of all the samples was detected by IHC. The results showed that the expression of Runx2 and OCN at the tendon-bone interface in each group gradually increased with time, but, more meaningfully, the proportion of positive cells at the tendon-bone

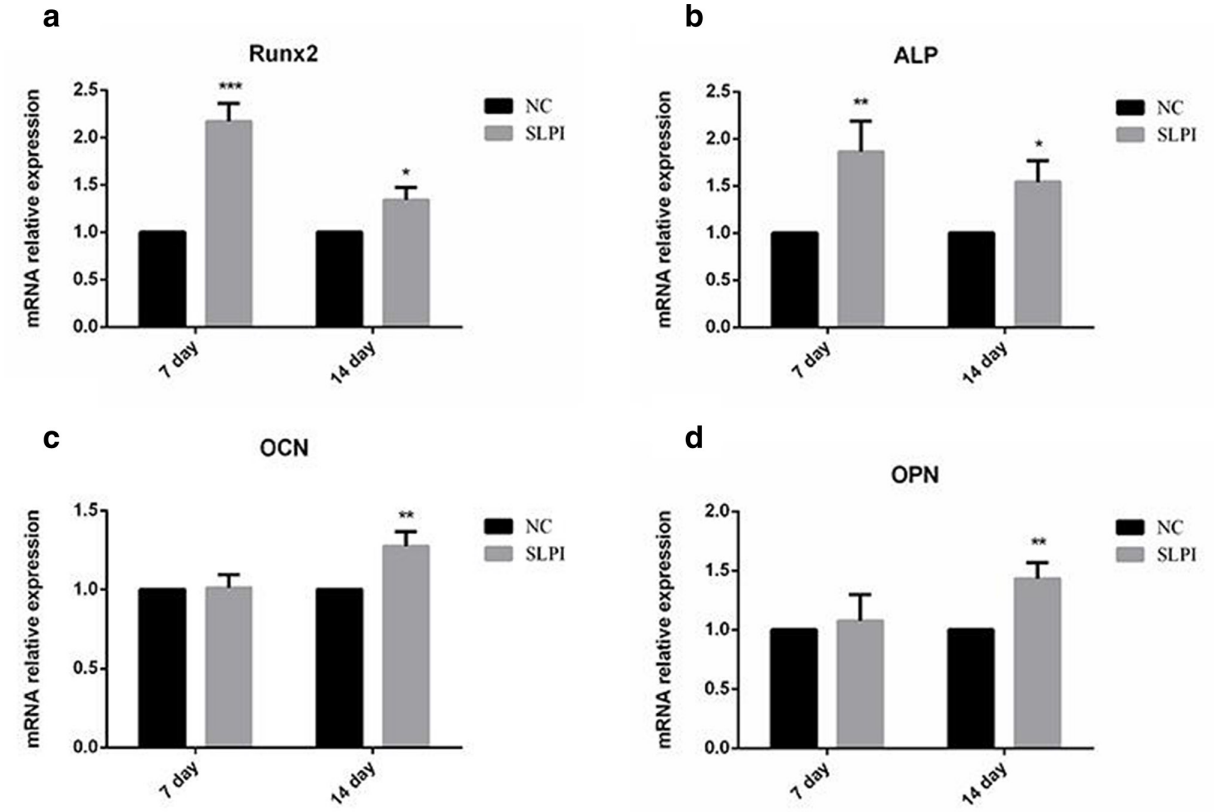

Fig. 4

After seven and 14 days of osteogenic induction, the levels of a) runt-related transcription factor 2 (Runx2), b) alkaline phosphatase (ALP), c) osteocalcin (OCN), and d) osteopontin (OPN) were measured by quantitative polymerase chain reaction (qPCR) (n = 3). Secretory leucocyte protease inhibitor (SLPI) increased the expression of Runx2, ALP, OCN, and OPN at different stages of osteogenic differentiation of bone mesenchymal stem cells (BMSCs). Runx2 and ALP increased significantly in the early stage of induction while OCN and OPN were upregulated in the more advanced stage of osteogenic induction. *p < 0.05; **p < 0.01; and ***p < 0.001. mRNA, messenger RNA; NC, negative control.

site of the SLPI group was significantly higher than in the NC group at all timepoints. The results were analyzed by comparing the number of positive cells as a percentage of the total cells of the tendon-bone connection in each high-magnification field (×200 and ×400) (Figure 5).

Histological evaluation. Histological analyses were performed to assess bone formation, cartilage formation, and tendon-bone connection. The staining results show that at the two weeks after ACL reconstruction, both of the two groups exhibited a fibrovascular connective tissue interface between tendon and bone, while there was more continuous new bone formation around the grafted tendon in the SLPI group (Figures 6a and 6b). At four weeks, the SLPI group showed more new bone ingrowth and tendon remodelling compared to the NC group; chondrocytes were present in some samples (Figures 6a and 6b). The SLPI group exhibited a smooth transition structure with more cartilage-like cell formation at eight weeks after operation (Figures 6a and 6b). At each timepoint after operation, the SLPI group had more chondrocytes than the NC group (Figure 6c). The tendon-bone interface was scored by three observers (DX, YS, JY) in both the SLPI group and the NC group, and the scores of the SLPI group were found to be significantly higher than those of the NC group at four ($p = 0.024$) and eight weeks ($p = 0.007$) (Figure 7).

Micro-CT analysis. Results of micro-CT scanning (Figure 8a) showed that the tunnel cross-sectional area (mm^2) of all animals decreased with time, but the bone tunnel of the SLPI group had a smaller cross-sectional area than the NC group at four weeks ($p = 0.038$) and eight weeks ($p = 0.008$). At four weeks ($p = 0.042$) and eight weeks ($p = 0.035$) after ACL reconstruction, BV/TV (%) indicated that new bone formation around the graft tendon was higher in the SLPI group at two weeks, but this difference was not statistically significant ($p = 0.058$); BMD (mg hydroxyapatite-cm^3), which represents new bone mineralization, was dramatically increased at eight weeks in the SLPI group compared with the NC group ($p = 0.033$), while there was no significant difference at four weeks ($p = 0.191$; Figure 8b).

Biomechanical testing. The biomechanical strength of the tendon-bone connection after ACL reconstruction was evaluated by recording and analyzing the maximum tensile force and stiffness of the ligaments using a biomechanical test system. At eight weeks postoperatively, the mean maximum tensile force (30.79 N (SD 2.958)) and mean stiffness (1.880 N/mm (SD 0.2395)) of the SLPI

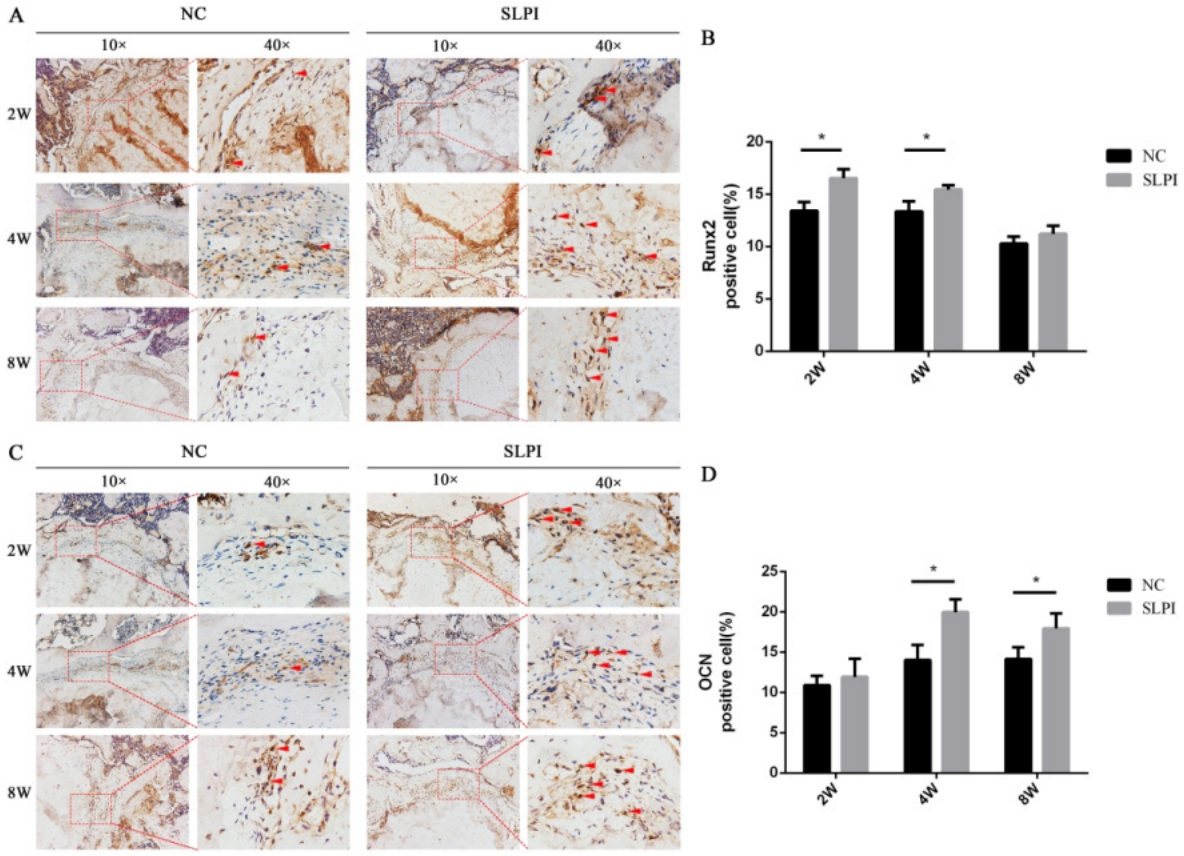

Fig. 5

a) The expression of runt-related transcription factor 2 (Runx2) at the tendon-bone interface at two, four, and eight weeks in each of the two groups (n = 4) using 3, 3 -diaminobenzidine (DAB) staining, and b) the proportion of Runx2-positive cells quantified at a magnification of ×400. Results are presented as mean and standard deviation (SD). *p < 0.05. c) Expression of osteocalcin (OCN) at the tendon-bone junction at two, four, and eight weeks in each of the two groups (n = 4). d) The proportion of OCN-positive cells was quantified at a magnification of ×400. Results are presented as mean and SD. *p < 0.05. NC, negative control; SLPI, secretory leucocyte protease inhibitor.

group were greater than those of the NC group (24.72 N (SD 2.778) and (1.461 N/mm (SD 0.1421)), with statistically significant differences (p = 0.024 and p = 0.023, respectively; Figures 2b and 2c). In comparison, the maximum failure tension and stiffness of the intrinsic ACL were 23.13 N (SD 3.064) and 2.36 N/mm (SD 0.3674), respectively.

Discussion

Many factors determine the outcome of ACL reconstruction, including the graft fixation, graft mechanical load, and graft materials, but the most important factor is firm healing between tendon and bone.[25,26] In our research, we illustrated that the delivery of rSLPI by fibrin gel into the bone tunnel promoted chondrogenesis and osteogenic differentiation at the tendon-bone interface, thereby increasing the cartilage and bone formation, enhancing the biological strength of tendon-bone connection, and finally accelerating the tendon-to-bone healing after ACL reconstruction in rat. Our study underlines the high value of SLPI in tendon-bone recovery, and points to SLPI injection as an effective therapy for ACL ruptures.

ACL tears are some of the most common sports injuries, due to the concentration of stress at the tendon-bone connecting area, which is prone to rupture.[27–29] Currently, the most effective means of treating injuries in the tendon-bone junction is surgical reconstruction.[30,31] However, second ACL injury rates of 23% have been reported, especially in the early return-to-sport period.[32] In the normal tendon-bone junction, a transitional four-layer structure of bone-mineralized cartilage-unmineralized cartilage-tendon is necessary for buffering the force aligning the muscles to bone. However, due to a poor self-healing ability,[17] once the tendon-bone junction is injured, a large amount of scar tissue is formed at the tendon-bone interface during the healing process instead of the typical four-layer structure.[33] The poor biomechanical strength of the scar tissue leads to a considerable decrease in mechanical properties after healing, which is one of the main reasons for poor recovery after ACL reconstruction.[17,34] Hence, it is crucial to find a better way to restore the intrinsic structure of the ACL. For the first time, we determined that SLPI could effectively accelerate the process of tendon-bone healing, and enhance the

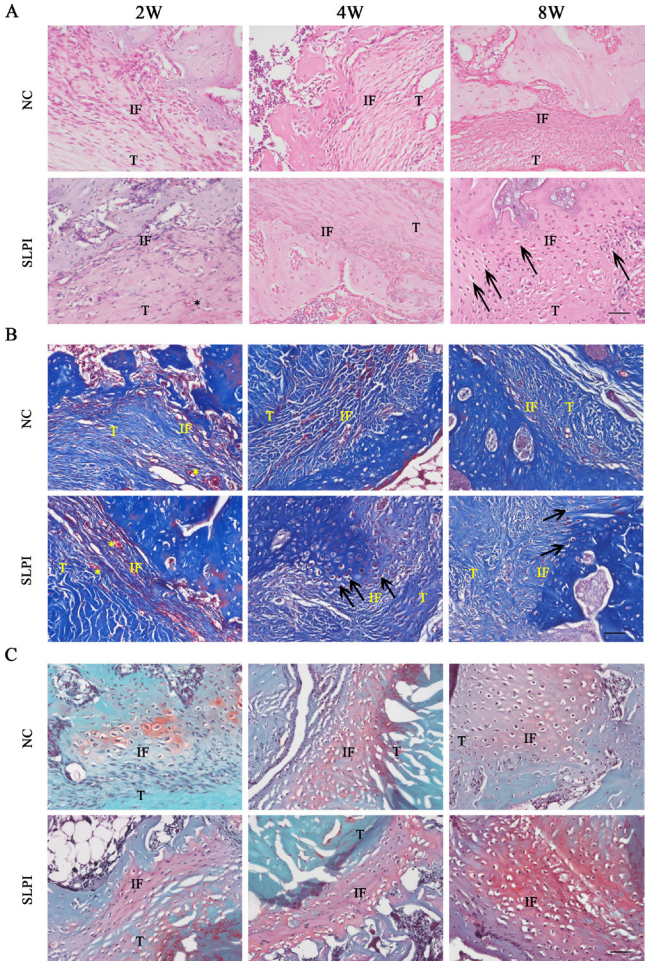

Fig. 6

a) Haemotoxylin and eosin (H&E) staining of the tendon-bone interface at two, four, and eight weeks after surgery in the secretory leucocyte protease inhibitor (SLPI) and negative control (NC) groups, respectively (n = 4). b) Masson's trichrome staining of the tendon-bone interface of samples at two, four, and eight weeks in the SLPI and NC groups, respectively (n = 4). c) Modified Safranin-O/Fast Green staining of the tendon-bone interface at two, four, and eight weeks in the SLPI and NC groups, respectively (n = 4). IF, interface; T, tendon; arrow: cartilage-like cell, asterisk: neovascularization; bar 20 μm.

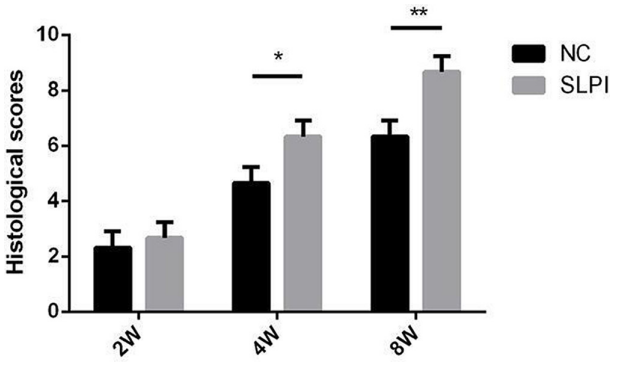

Fig. 7

Mean histological scores (standard deviations) of the tendon-bone interface in the study group (SLPI, secretory leucocyte protease inhibitor) and the control group (NC, negative control) at two, four, and eight weeks after operation (n = 4). *p < 0.05; **p < 0.01.

strength of tendon-bone connection, which may serve as a potential therapeutic target in ACL rupture.

Since the strength of tendon-bone healing after ACL reconstruction depends on osseointegration between the tendon graft and bone,[10] recent attempts have been made to enhance the osseointegration of the tendon graft into the bone tunnel. SLPI has attracted the attention of many researchers in recent years. In mucosal tissues, SLPI inhibits proteases, prevents cell destruction, and maintains homeostasis, thus protecting against inflammation.[35] In the injured central nervous system, SLPI promotes axonal regeneration and functional recovery.[36] SLPI also plays an important role in cutaneous wound healing, and absence of SLPI in mice showed delayed wound repair and excessive inflammation.[37] Moreover, SLPI regulates the communication between osteoblasts and osteoclasts, promoting PTH-induced bone anabolism.[15] However, whether SLPI modulates these effects in tendon-bone healing remains unclear. In our study, in vitro experiments confirmed the ability of SLPI to promote the mobility and osteogenic differentiation of BMSCs, while in vivo experiments showed that SLPI promotes osteoblast formation in the early stage of tendon-bone healing after ACL reconstruction in a rat model, making the tendon-bone interface a beneficial microenvironment in the early stage of healing and allowing better tendon-bone healing in the later stage.

Zhang et al[38] used fibrin gel as a carrier injected into the bone tunnel after ACL reconstruction in a rabbit model. We also used fibrin gels as carriers with the aim of avoiding the possible degradation of exogenous proteins by the joint fluid. According to a rat model of ACL reconstruction, we found better histological outcomes after SLPI treatment carried by fibrin gel, which led to more new bone formation and mineralization around the graft and improved biomechanical properties.

However, there are several limitations to our study. First, we only investigated three timepoints which were at relatively early stages of the healing process, limiting our viability to show an effect of SLPI on later repair stages. Second, this experiment did not reveal the molecular mechanism of SLPI in promoting osteogenic differentiation, and it will be necessary to carry out further research to clarify the mechanism of the specific effect and the pathways involved. At present, the preparation process of SLPI is still complex and expensive, and further research may need to be done into SLPI before it can be used in clinical settings. Third, in future studies, the optimal concentration and sustained release system of rSLPI are worthy of further investigation to enhance tendon-bone interface healing. Fourth, although we have confirmed the promoting effect of rSLPI on ACL reconstruction using a rat model, rSLPI still cannot be applied directly to clinical surgery. It is necessary to carry out rigorous preclinical research in the future. Finally, research results

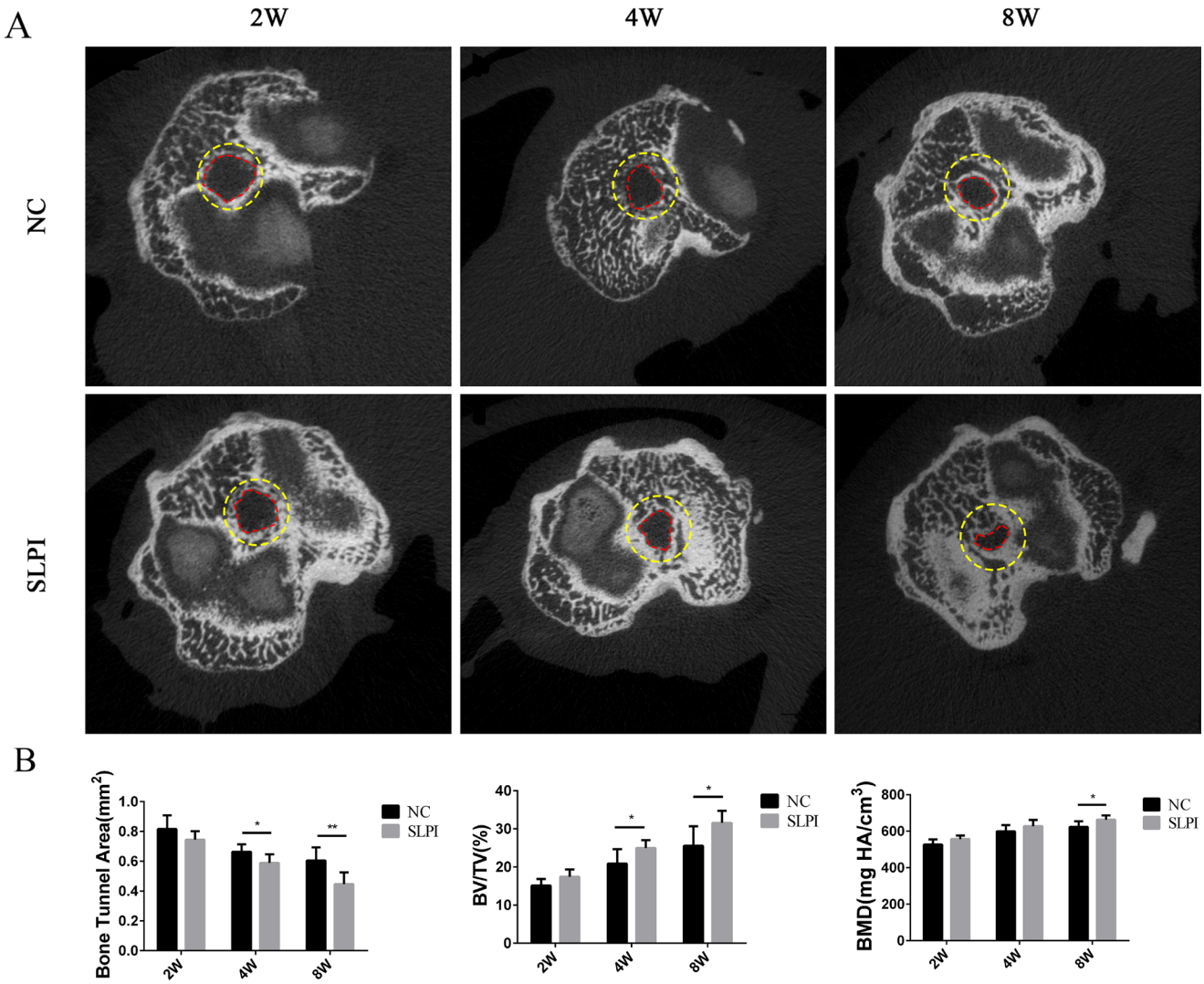

Fig. 8

a) Micro-CT was performed to evaluate the cross-sectional area of the tibial tunnel in the secretory leucocyte proteinase inhibitor (SLPI) and negative control (NC) groups at two, four, and eight weeks (n = 4). The planes (yellow dashed circle) were chosen at a depth of 5 mm from the tibial plateau. b) Results of bone tunnel area, bone volume/total volume (BV/TV (%)), and bone mineralization density (BMD) of the samples from each of the two groups at two, four, and eight weeks. The results are expressed as mean and standard deviations, *p < 0.05; **p < 0.01. The red dashed line indicates the outline of the bone tunnel.

may be biased, due to the limited number of samples and individual differences of animals.

In summary, SLPI reduces the formation of tissue scars and promotes osteogenic differentiation after recruiting BMSCs from the bone marrow cavity. Under the influence of the local microenvironment, SLPI accelerates the process of osteogenesis and increases osseointegration and bone mineralization around a graft, ultimately improving the strength of tendon-bone healing. Exogenous supplement of SLPI may serve as a potential therapy for tendon-bone interface reconstruction.

In conclusion, SLPI can enhance the migration and osteogenic differentiation of BMSCs in vitro, and also effectively promotes early tendon-bone healing after ACL reconstruction at eight weeks in vivo.

Supplementary material

In vitro drug release and sustainability analysis of secretory leucocyte protease inhibitor, and ARRIVE checklist.

References

1. **Śmigielski R**, **Zdanowicz U**, **Drwięga M**, **Ciszek B**, **Williams A**. The anatomy of the anterior cruciate ligament and its relevance to the technique of reconstruction. *Bone Joint J*. 2016;98-B(8):1020–1026.
2. **Hexter AT**, **Hing KA**, **Haddad FS**, **Blunn G**. Decellularized porcine xenograft for anterior cruciate ligament reconstruction: A histological study in sheep comparing cross-pin and cortical suspensory femoral fixation. *Bone Joint Res*. 2020;9(6):293–301.
3. **Scott CEH**, **Holland G**, **Krahelski O**, **Murray IR**, **Keating JF**, **Keenan OJF**. Patterns of cartilage loss and anterior cruciate ligament status in end-stage osteoarthritis of the knee. *Bone Joint J*. 2020;102-B(6):716–726.

4. **Yao S**, **Fu BS-C**, **Yung PS-H**. Graft healing after anterior cruciate ligament reconstruction (ACLR. *Asia Pac J Sports Med Arthrosc Rehabil Technol*. 2021;25:8–15.
5. **Dong Y**, **Zhang Q**, **Li Y**, **Jiang J**, **Chen S**. Enhancement of tendon-bone healing for anterior cruciate ligament (ACL) reconstruction using bone marrow-derived mesenchymal stem cells infected with BMP-2. *Int J Mol Sci*. 2012;13(10):13605–13620.
6. **Baksh D**, **Song L**, **Tuan RS**. Adult mesenchymal stem cells: characterization, differentiation, and application in cell and gene therapy. *J Cell Mol Med*. 2004;8(3):301–316.
7. **Gulotta LV**, **Kovacevic D**, **Ehteshami JR**, **Dagher E**, **Packer JD**, **Rodeo SA**. Application of bone marrow-derived mesenchymal stem cells in a rotator cuff repair model. *Am J Sports Med*. 2009;37(11):2126–2133.
8. **Nejadnik H**, **Hui JH**, **Feng Choong EP**, **Tai BC**, **Lee EH**. Autologous bone marrow-derived mesenchymal stem cells versus autologous chondrocyte implantation: an observational cohort study. *Am J Sports Med*. 2010;38(6):1110–1116.
9. **Hao Z-C**, **Wang S-Z**, **Zhang X-J**, **Lu J**. Stem cell therapy: a promising biological strategy for tendon-bone healing after anterior cruciate ligament reconstruction. *Cell Prolif*. 2016;49(2):154–162.
10. **Lu CC**, **Chou SH**, **Shen PC**, **Chou PH**, **Ho ML**, **Tien YC**. Extracorporeal shock wave promotes activation of anterior cruciate ligament remnant cells and their paracrine regulation of bone marrow stromal cells' proliferation, migration, collagen synthesis, and differentiation. *Bone Joint Res*. 2020;9(8):458–468.
11. **Antoniades CG**, **Khamri W**, **Abeles RD**, **et al**. Secretory leukocyte protease inhibitor: a pivotal mediator of anti-inflammatory responses in acetaminophen-induced acute liver failure. *Hepatology*. 2014;59(4):1564–1576.
12. **Wagenblast E**, **Soto M**, **Gutiérrez-Ángel S**, **et al**. A model of breast cancer heterogeneity reveals vascular mimicry as a driver of metastasis. *Nature*. 2015;520(7547):358–362.
13. **Vigo T**, **La Rocca C**, **Faicchia D**, **et al**. IFNβ enhances mesenchymal stromal (Stem) cells immunomodulatory function through STAT1-3 activation and mTOR-associated promotion of glucose metabolism. *Cell Death Dis*. 2019;10(2):85.
14. **Munn LL**, **Garkavtsev I**. SLPI: a new target for stopping metastasis. *Aging (Albany NY)*. 2018;10(1):13–14.
15. **Morimoto A**, **Kikuta J**, **Nishikawa K**, **et al**. SLPI is a critical mediator that controls PTH-induced bone formation. *Nat Commun*. 2021;12(1):2136.
16. **Takamura T**, **Suguro H**, **Mikami Y**, **et al**. Comparison of gene expression profiles of gingival carcinoma Ca9-22 cells and colorectal adenocarcinoma HT-29 cells to identify potentially important mediators of SLPI-induced cell migration. *J Oral Sci*. 2017;59(2):279–287.
17. **Bakirci E**, **Tschan K**, **May RD**, **Ahmad SS**, **Kleer B**, **Gantenbein B**. The importance of plasmin for the healing of the anterior cruciate ligament. *Bone Joint Res*. 2020;9(9):543–553.
18. **Jeong S-J**, **Wang G**, **Choi B-D**, **et al**. Secretory Leukocyte Protease Inhibitor (SLPI) Increases Focal Adhesion in MC3T3 Osteoblast on Titanium Surface. *J Nanosci Nanotechnol*. 2015;15(1):200–204.
19. **Gao T**, **Liu X**, **He B**, **Pan Y**, **Wang S**. Long non-coding RNA 91H regulates IGF2 expression by interacting with IGF2BP2 and promotes tumorigenesis in colorectal cancer. *Artif Cells Nanomed Biotechnol*. 2020;48(1):664–671.
20. **Bobadilla AVP**, **Arévalo J**, **Sarró E**, **et al**. In vitro cell migration quantification method for scratch assays. *J R Soc Interface*. 2019;16(151):20180709.
21. **Kawakami Y**, **Takayama K**, **Matsumoto T**, **et al**. Anterior cruciate ligament-derived stem cells transduced with BMP2 accelerate graft-bone integration after ACL reconstruction. *Am J Sports Med*. 2017;45(3):584–597.
22. **Nakano N**, **Matsumoto T**, **Takayama K**, **et al**. Age-dependent healing potential of anterior cruciate ligament remnant-derived cells. *Am J Sports Med*. 2015;43(3):700–708.
23. **Chen B**, **Li B**, **Qi Y-J**, **et al**. Enhancement of tendon-to-bone healing after anterior cruciate ligament reconstruction using bone marrow-derived mesenchymal stem cells genetically modified with bFGF/BMP2. *Sci Rep*. 2016;6:25940.
24. **Yeh W-L**, **Lin S-S**, **Yuan L-J**, **Lee K-F**, **Lee MY**, **Ueng SWN**. Effects of hyperbaric oxygen treatment on tendon graft and tendon-bone integration in bone tunnel: biochemical and histological analysis in rabbits. *J Orthop Res*. 2007;25(5):636–645.
25. **Camp CL**, **Lebaschi A**, **Cong G-T**, **et al**. Timing of postoperative mechanical loading affects healing following anterior cruciate ligament reconstruction: analysis in a murine model. *J Bone Joint Surg Am*. 2017;99-A(16):1382–1391.
26. **Hjorthaug GA**, **Madsen JE**, **Nordsletten L**, **Reinholt FP**, **Steen H**, **Dimmen S**. Tendon to bone tunnel healing--a study on the time-dependent changes in biomechanics, bone remodeling, and histology in a rat model. *J Orthop Res*. 2015;33(2):216–223.
27. **Xerogeanes JW**, **Hammond KE**, **Todd DC**. Anatomic landmarks utilized for physeal-sparing, anatomic anterior cruciate ligament reconstruction: an MRI-based study. *J Bone Joint Surg Am*. 2012;94-A(3):268–276.
28. **Siegel L**, **Vandenakker-Albanese C**, **Siegel D**. Anterior cruciate ligament injuries: anatomy, physiology, biomechanics, and management. *Clin J Sport Med*. 2012;22(4):349–355.
29. **Nogaro M-C**, **Abram SGF**, **Alvand A**, **Bottomley N**, **Jackson WFM**, **Price A**. Paediatric and adolescent anterior cruciate ligament reconstruction surgery. *Bone Joint J*. 2020;102-B(2):239–245.
30. **Kayani B**, **Konan S**, **Ahmed SS**, **Chang JS**, **Ayuob A**, **Haddad FS**. The effect of anterior cruciate ligament resection on knee biomechanics. *Bone Joint J*. 2020;102-B(4):442–448.
31. **Stockton DJ**, **Schmidt AM**, **Yung A**, **et al**. Tibiofemoral contact and alignment in patients with anterior cruciate ligament rupture treated nonoperatively versus reconstruction : an upright, open MRI study. *Bone Joint J*. 2021;103-B(9):1505–1513.
32. **Wiggins AJ**, **Grandhi RK**, **Schneider DK**, **Stanfield D**, **Webster KE**, **Myer GD**. Risk of secondary injury in younger athletes after anterior cruciate ligament reconstruction: a systematic review and meta-analysis. *Am J Sports Med*. 2016;44(7):1861–1876.
33. **Chen Y**, **Xu Y**, **Li M**, **Shi Q**, **Chen C**. Application of autogenous urine-derived stem cell sheet enhances rotator cuff healing in a canine model. *Am J Sports Med*. 2020;48(14):3454–3466.
34. **Han F**, **Zhang P**, **Chen T**, **Lin C**, **Wen X**, **Zhao P**. A LbL-assembled bioactive coating modified nanofibrous membrane for rapid tendon-bone healing in ACL reconstruction. *Int J Nanomedicine*. 2019;14:9159–9172.
35. **Tang R**, **Botchway BOA**, **Meng Y**, **et al**. The inhibition of inflammatory signaling pathway by secretory leukocyte protease inhibitor can improve spinal cord injury. *Cell Mol Neurobiol*. 2020;40(7):1067–1073.
36. **Hannila SS**. Secretory Leukocyte Protease Inhibitor (SLPI): emerging roles in CNS trauma and repair. *Neuroscientist*. 2015;21(6):630–636.
37. **Ashcroft GS**, **Jeong M-J**, **Ashworth JJ**, **et al**. Tumor necrosis factor-alpha (TNF-α) is a therapeutic target for impaired cutaneous wound healing. *Wound Repair Regen*. 2012;20(1):38–49.
38. **Zhang X**, **Ma Y**, **Fu X**, **et al**. Runx2-modified adipose-derived stem cells promote tendon graft integration in anterior cruciate ligament reconstruction. *Sci Rep*. 2016;6:19073.

Author information:

- Y. Wu, MM, Orthopaedic Surgeon, Department of Orthopedics, Orthopedic Hospital of Guangdong Province, Academy of Orthopedics, The Third Affiliated Hospital of Southern Medical University, Guangzhou, China; The Third School of Clinical Medicine, Southern Medical University, Guangzhou, China; Guangdong Provincial Key Laboratory of Bone and Joint Degeneration Diseases, Guangzhou, China; Department of Orthopedics, Fourth Affiliated Hospital of Guangxi Medical University/ Liuzhou Workers' Hospital, Liuzhou, China.
- Y. Shao, PhD, Orthopaedic Surgeon
- D. Xie, MD, PhD, Orthopaedic Surgeon
- J. Pan, MM, Orthopaedic Surgeon
- D. Cai, MD, PhD, Orthopaedic Surgeon
- C. Zeng, MD, PhD, Orthopaedic Surgeon
  Department of Orthopedics, Orthopedic Hospital of Guangdong Province, Academy of Orthopedics, The Third Affiliated Hospital of Southern Medical University, Guangzhou, China; The Third School of Clinical Medicine, Southern Medical University, Guangzhou, China; Guangdong Provincial Key Laboratory of Bone and Joint Degeneration Diseases, Guangzhou, China.
- H. Chen, MD, Postdoctoral Candidate
- J. Yao, MM, Graduate Student
- J. Liang, MM, Graduate Student
- H. Ke, MM, Graduate Student
  Department of Orthopedics, Orthopedic Hospital of Guangdong Province, Academy of Orthopedics, The Third Affiliated Hospital of Southern Medical University, Guangzhou, China; The Third School of Clinical Medicine, Southern Medical University, Guangzhou, China.

Author contributions:

- Y. Wu: Conceptualization, Formal analysis, Investigation, Methodology, Writing – original draft, Writing – review & editing.
- Y. Shao: Methodology, Resources, Visualization.
- D. Xie: Validation, Investigation.
- J. Pan: Data curation, Resources.
- H. Chen: Writing – review & editing.
- J. Yao: Software.
- J. Liang: Validation.
- H. Ke: Validation.
- D. Cai: Project administration, Supervision.
- C. Zeng: Supervision, Funding acquisition, Project administration.

- Y. Wu, Y. Shao, and D. Xie contributed equally to this work.

- D. Cai and C. Zeng contributed equally to this work.

Funding statement:
- The authors disclose receipt of the following financial or material support for the research, authorship, and/or publication of this article: financial support from the National Natural Science Foundation of China (No. 81974327), the Natural Science Foundation of Guangdong Province (No.2018A030313278), and the Natural Science Foundation of Guangdong Province (No.2022A1515011101).

Acknowledgements:
- We would like to give our sincere appreciation to the reviewers for their helpful comments to this article.

Ethical review statement:
- Animal experiments in this study were conducted in compliance with nationally or internationally recognized guidelines, and approved by the Animal Ethics Committee of Southern Medical University, Guangzhou, China.

Open access funding
- The open access fee was funded by the grants mentioned above.